Check for updates

Resistance to CLnA-induced ferroptosis is acquired in Caco-2 cells upon differentiation

Géraldine Cuvelier[1†], Perrine Vermonden[1†], Justine Rousseau[1], Olivier Feron[2], René Rezsohazy[1] and Yvan Larondelle[1]*

[1]Louvain Institute of Biomolecular Science and Technology, UCLouvain, Walloon Brabant, Belgium,
[2]FATH, Institut de Recherche Expérimentale et Clinique, UCLouvain, Brussels, Belgium

In contrast to canonical ferroptosis inducers, highly peroxidable conjugated linolenic acids (CLnA) directly fuel the lipid peroxidation cascade upon their incorporation into membrane phospholipids. Little is known, however, about the cytotoxicity level of CLnAs to normal epithelial cells. Caco-2 cells, derived from colorectal adenocarcinoma, spontaneously differentiate into enterocyte-like cells over a period of 21 days of cell culturing, allowing for graduated phenotypic shift from proliferative, undifferentiated cells to a functional intestinal barrier. We exploited this property to assess the sensitivity of Caco-2 cells to CLnAs at different stages of differentiation. Our results show a significant decrease in CLnA-induced ferroptotic cell death over time. The acquired resistance aligned with decreases in cell proliferation and in the extent of lipid peroxidation, as well as with an increase in the expression of GPX4 upon differentiation. These results highlight that while CLnAs are highly toxic for proliferating cancer cells, differentiated epithelial cells are resistant to CLnA-induced ferroptosis. Therefore, this study gives credential to the therapeutic use of CLnAs as an anticancer strategy and offers a new model study to further investigate the safety of peroxidable fatty acids in differentiated cells.

KEYWORDS

conjugated linolenic acids (CLnAs), cell differentiation, ferroptosis, lipid peroxidation, cancer, Caco-2 cells

1 Introduction

For a long time, promoting apoptosis has been the main focus of anticancer drug discovery. More recently, among other types of cell death, ferroptosis has emerged as a potential target to overcome drug resistance (Dixon et al., 2012). This iron-dependent regulated cell death is triggered by the lethal accumulation of lipid hydroperoxides inside the cell. Its occurrence is due to a cellular systematic imbalance between the production of lipid hydroperoxides and the antioxidant repair systems. Lipid hydroperoxides emerge from enzymatic and non-enzymatic oxidation of polyunsaturated fatty acids (PUFAs) contained in membrane phospholipids. Non-enzymatic oxidation of membrane phospholipids is facilitated by reactive oxygen species (ROS) arising from the Fenton reaction while enzymatic oxidation relies on iron-dependent enzymes, such as lipoxygenase (Chu et al., 2019), NADPH oxidase (NOX) (Xie et al., 2017) and cytochrome P450 (POR) (Xie et al., 2017; Zou et al., 2020).

The cellular antioxidant defenses are based on three lipid peroxide detoxifying systems. Glutathione peroxidase 4 (GPX4) and its substrate glutathione (GSH) were the first to be

discovered and hold a major role in the detoxification of lipid hydroperoxides. The other ferroptosis suppressive systems consist of ferroptosis suppressor protein (FSP1) and dihydrofolate reductase (DHFR) and their respective substrates, Coenzyme Q10 (CoQ10) and tetrahydrobiopterin (BH4). Ferroptosis sensitivity is also negatively influenced by cell density via the Hippo pathway that is activated by E-cadherin (ECAD). Accordingly, for a given cancer cell line, high-density seeding was associated with more resistance to ferroptosis induction than low-density cell cultures (Wu et al., 2019; Yang et al., 2019).

While in healthy cells, the production of lipid hydroperoxides is counteracted by potent antioxidant systems, uncontrolled cancer cell proliferation accounts for exacerbated cellular metabolism leading to high ROS production (Pavlova and Thompson, 2016; Bian et al., 2021). Therefore, disrupting the iron metabolism or antioxidant defense systems through chemical induction alters the detoxification of lipid hydroperoxides to a larger extent in cancer cells (Liang et al., 2019). Several low molecular weight drugs are currently under study for their ability to inhibit critical substrates or enzymes related to the three major anti-ferroptotic pathways indicated above. For instance, RSL3 and Erastin are two drugs used to pharmacologically induce ferroptosis either through direct GPX4 inhibition or through the blockade of glutathione import via the xCT glutamate-cystine antiporter (Liang et al., 2019). The high energy requirements of cancer cells may also be exploited to promote the uptake of exogenous PUFAs, the substrate for peroxidation in cell membranes. Indeed, high amounts of PUFA-containing phospholipids increase the susceptibility of cells toward ferroptosis. Acyl-CoA synthetase long chain family member 4 (ACSL4) was among the first ferroptotic biomarkers to be discovered (Doll et al., 2017). Together with lysophosphatidylcholine acyltransferase (LPCAT3), it activates and integrates newly synthesized or imported PUFAs into cell membranes.

Several lines of research suggest that enhanced ferroptosis sensitivity can be achieved by supplementing cancer cells with n-3, n-6 and other types of PUFAs (Kagan et al., 2017; Dierge et al., 2020; Perez et al., 2020). We and others highlighted the efficacy of α-eleostearic acid (αESA), jacaric acid (JA) and punicic acid (PunA), three structure-related PUFAs, to trigger ferroptosis in cancer cells (Shinohara et al., 2012; Beatty et al., 2019; Vermonden et al., 2021). These fatty acids belong to the family of conjugated linolenic acids (CLnAs) of plant origin. The presence of three conjugated double bonds renders these molecules highly prone to peroxidation, thereby representing valuable candidates for alternative ferroptosis induction (Dhar Dubey et al., 2019). Seven isomers of plant-derived CLnAs are naturally present in nature. Two of them, PunA and αESA, are present in human-consumed food items: PunA is found in the seeds of *Punica granatum*, and represents up to 80% of all fatty acids of pomegranate seed oil (PSO); αESA represents up to 50% of all the fatty acids present in *Ricinodendron heudelotii* seeds consumed in several central African countries (Leudeu et al., 2009). The last CLnA of interest in the current study, JA, known to be the most cytotoxic of all CLnAs (Beatty et al., 2021), is found in seeds of *Jacaranda mimosifolia*, a tree which grows in subtropical regions. Of these isomers, only a few *in vivo* studies showing the safety of consumption of pomegranate seed oil (PSO) and ricinodendron seeds have been carried out so far and no *in vitro*

studies evaluating the safety of CLnAs for normal cells exist (Meerts et al., 2009). Investigating the impact of PunA, JA and αESA on *in vitro* healthy cell models would fill the gap of knowledge between their impact on cancer cells *in vitro* and their safe use *in vivo*.

Caco-2 cells represent an interesting cancer cell line that may be differentiated *in vitro*. Indeed, Caco-2 cells, derived from a colorectal adenocarcinoma, are characterized by their ability to spontaneously differentiate over time when cultured as monolayers. After 21 days of culturing, Caco-2 cells form a functional enterocyte-like barrier composed of differentiated epithelial cells able to absorb nutrients at the apical brush border and to release the absorbed nutrients at the basolateral border (Natoli et al., 2012).

In the present work, we explore the cytotoxicity of CLnAs using differentiating Caco-2 cells as a model. The results show that Caco-2 cells become resistant to CLnAs upon differentiation. This acquired resistance can be linked to decreased lipid peroxidation and increased expression of GPX4, further highlighting the importance of the GPX4 antioxidant system as a protective mechanism against ferroptosis.

2 Materials and methods

2.1 Cell culture and chemicals

Caco-2 cells, derived from a colon adenocarcinoma, were obtained from DSMZ and were cultured from passage 32 to 39 in DMEM containing 4.5 g/L glucose (Gibco) supplemented with 2 mM L-glutamine, 1 mM sodium pyruvate, 1% (v/v) non-essential amino acids (NEAA), 1% (v/v) penicillin/streptomycin and 10% (v/v) heat-inactivated FBS in an atmosphere of 90% air/10% CO_2 (v/v) at 37°C. Cells were negatively tested for *mycoplasma* contamination prior to the study using the MycoAlert detection kit (Lonza). 6-, 48- and 96-well plates were used for cell growth and each well was systematically coated with 1% of sterile type-I collagen (Sigma, C8919) for 1 h at 37°C prior to seeding. The culture medium was changed every 2–3 days. All the fatty acids used in the experiments were purchased from Larodan: stearic acid (STE, 10-1800), oleic acid (OLE, 10-1801), alpha-linolenic acid (ALA, 10-1803), docosahexaenoic acid (DHA, 10-2206), punicic acid (PunA, 10-1875), jacaric acid (JA, 10-1876) and alpha-eleostearic acid (αESA, 10-1871). The fatty acids used to treat the cells were conjugated to albumin in a 4:1 ratio (w/w) and dissolved in phosphate buffer saline before being stored at −80°C in aliquots. Ferrostatin-1 (fer-1, Sigma Aldrich, SML0583) and RSL3 (Selleck Chemicals, S8155) were dissolved in DMSO. Cell viability assessment was performed using PrestoBlue™ cell viability reagent (Fisher Scientific, 12083745).

2.2 Cell viability assessment

For cell differentiation related viability assays, cells were cultured in 48-well plates and seeded at a density of 60,000 cells/well. The timeline for cell differentiation started 24 h after seeding. From day 0 to day 21 of cell differentiation, cells were treated every 2 or 3 days with 7 different fatty acids, varying in degree of unsaturation, at a concentration of 100 μM. Three additional conditions combining

fer-1 at 10 μM and one of the 3 CLnAs at 100 μM were used for the assay. For dose-response related cell viability assays, cells were cultured in 96-well plates at a seeding density of 27,000 cells/well to preserve the surface ratio with cells grown in 48-well plates. Cells were treated at day 2 of cell differentiation with increasing concentrations of PunA, JA or αESA or with the canonical ferroptotic inhibitor RSL3. For both experiments, after 72 h of treatment, cell viability was assessed with PrestoBlue™ reagent, which assesses the amount of living cells based on their capability to reduce non fluorescent blue resazurin contained in the reagent into resorufin, an intensively red-fluorescent dye according to manufacturer's instructions.

2.3 Measurement of lipid peroxidation

Cells were seeded at a density of 15,000 cells/well in 96-well black/clear bottom plates (Greiner Bio One, 655090). Cells were treated with the 7 different fatty acids at a concentration of 100 μM, the 3 CLnAs being applied on cells either with or without fer-1 10 μM. Lipid peroxidation was measured after 12 h by adding 5 μM of the lipid peroxidation sensor C11-BODIPY 581/591 (4,4-difluoro-5-(4-phenyl-1,3-butadienyl)-4bora-3a,4a-diaza-s-indacene-3-undecanoic acid, Fisher Scientific, D3861). The probe contains 2 double bonds, which are oxidized in the presence of lipid ROS, thereby inducing a shift in fluorescence from red (excitation = 580 nm, emission = 620 nm) to green (excitation = 500 nm, emission = 540 nm) that was measured using the fluorometer Infinite Mpro200 plate reader (Tecan). Relative fluorescence, obtained upon division of the green fluorescence by the red fluorescence was used to measure the intracellular peroxidation level. The value obtained was then further divided by the value of the control condition to obtain a fold change expression.

2.4 Immunoblotting

Cells were seeded at a density of 480,000 cells/well in a 6-well plate. Cells were incubated with 100 μM of each of the 7 fatty acids for 24 h. The dose was selected based on the results from dose-response curves and the timing was chosen in order to prevent cell death from occurring at the time of cell collection. After 24 h, cells were washed twice with ice-cold PBS before being lysed in a RIPA buffer supplemented with a protease inhibitor cocktail for 5 min. The cell lysates were then collected and centrifuged at 16,000 rcf for 10 min. Finally, the supernatant was retrieved and stored at −80°C until bicinchoninic acid protein assay (Thermo Fisher Scientific, 23225) and Western blot were performed. Loadings were prepared by mixing a defined volume of sample to achieve 20 μg of proteins with an equal volume of Laemmli buffer. Samples were denatured for 5 min at 95°C before being loaded on a 10% SDS-PAGE gel. After 1 h migration at 120 V, the gel was transferred in a Mini TransBlot electrophoretic Transfer Cell using a PVDF membrane (VWR, NEF1002001PK), previously activated in methanol, for 45 min at a constant intensity of 350 mA. Membranes were then blocked in 5% skimmed milk-containing TTBS for 1 h at room temperature (RT) under constant shaking. Afterwards, the membranes were incubated at 4°C overnight under constant shaking with the following primary antibodies, diluted in 5% skimmed milk-containing TTBS: anti-

ACSL4 (Abcam, ab110007, 1:1000), anti-Cyclin A2 (Cell Signaling Technology, 67955, 1:1000), anti-DPP4 (Cell Signaling Technology, 67138, 1:1000), anti-GPX4 (Abcam, ab125066, 1:1000), anti-β-Actin (Merck, A5441, 1:10000), anti-VCP (Cell Signaling Technology, 2648, 1: 1000). The next day, membranes were washed 3 times in TTBS and were incubated with horseradish peroxidase-conjugated secondary antibodies (Cell Signaling Technology, anti-rabbit 7074, anti-mouse 7076) in 5% skimmed milk-containing TTBS for 1 h at RT. Finally, the secondary antibody was discarded, membranes were washed 3 times in TTBS and the chemiluminescent signal was read after addition of Amersham ECL detection reagent (VWR, RPN2134) with a chemiluminescence Amershan Imager 600 (Cytiva).

2.5 Statistics

GraphPad Prism 9.1 software was used to perform statistical analysis by using either one-way or two-way ANOVA with Sidak's multiple comparison tests. Statistical significance to the control or to another treatment is determined as follows: $*p \leq 0.05$; $**p \leq 0.01$; $***p \leq 0.001$; $****p \leq 0.0001$, with p being the p-value adjusted for multiple comparisons.

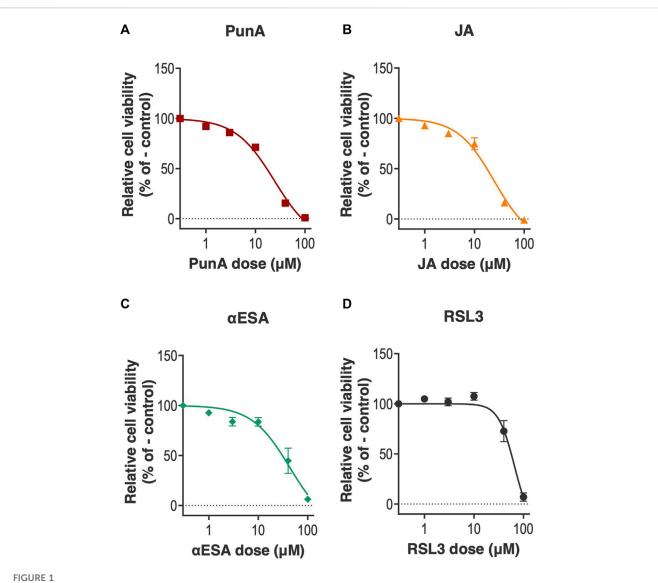# 3 Results

3.1 CLnAs are cytotoxic for undifferentiated Caco-2 cells

The viability of Caco-2 cells was assessed after 2 days of cell culture (referred to as day 2) when treated with increasing doses of three different CLnAs, namely, PunA, JA or αESA, or of the ferroptosis inducer RSL3 (Figure 1). All three CLnAs were cytotoxic to Caco-2 cells, with lethal doses LD50 of 23.99 ± 5.42, 24.75 ± 5.34 and 43.34 ± 8.68 μM for PunA, JA and αESA, respectively (Figures 1A–C). Interestingly, the addition of oleic acid (OLE), a monounsaturated fatty acid with anti-ferroptotic potential (Magtanong et al., 2019), did not significantly impact JA cytotoxicity on Caco-2 cells (Supplementary Figure S1), supporting its strong effect as pro-ferroptotic fatty acid. Similarly to CLnAs, RSL3 was also cytotoxic to Caco-2 cells, with an LD50 of 65.59 ± 6.95 μM (Figure 1D). Of note, Caco-2 cells at day 2 appeared to be relatively resistant to RSL3-driven ferroptosis when compared to other colorectal cancer cell lines (Doll et al., 2017; Xie et al., 2017; Doll et al., 2019). It should however be emphasized that the latter studies were conducted on cancer cells at high proliferation rates (i.e., corresponding to the day 0 in the present study) (Xie et al., 2017), while our results were obtained on Caco-2 cells already engaged in the process of cell differentiation (i.e., day 2) and thus at an already reduced proliferation rate.
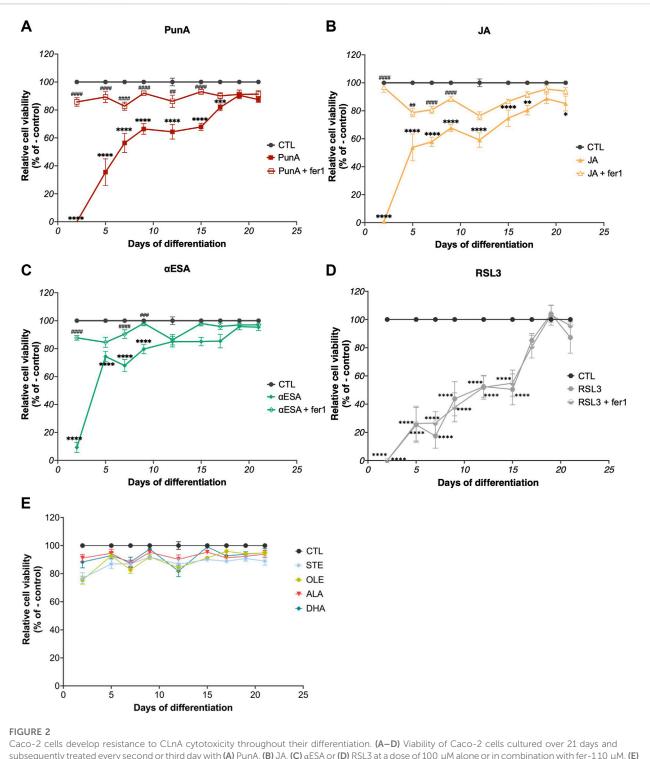
3.2 Differentiating Caco-2 cells develop increased resistance to CLnA-induced ferroptosis

Caco-2 cells were cultured over 21 days in order to differentiate into enterocytes and were exposed to different

FIGURE 1
CLnAs and RSL3 are cytotoxic to Caco-2 cells at 2 days of cell culture. **(A–D)** Viability of Caco-2 cells cultured for 2 days before treatment with increasing doses of **(A)** PunA, **(B)**, JA, **(C)** αESA or **(D)** RSL3 for 72 h. Results are expressed as mean ± standard error of the mean of three independent repetitions. Dose-response curves have been fitted to the data. Abbreviations: CLnA, Conjugated linolenic acids; αESA, α-eleostearic acid; JA, jacaric acid, PunA, punicic acid, RSL3, Ras-selective lethal 3.
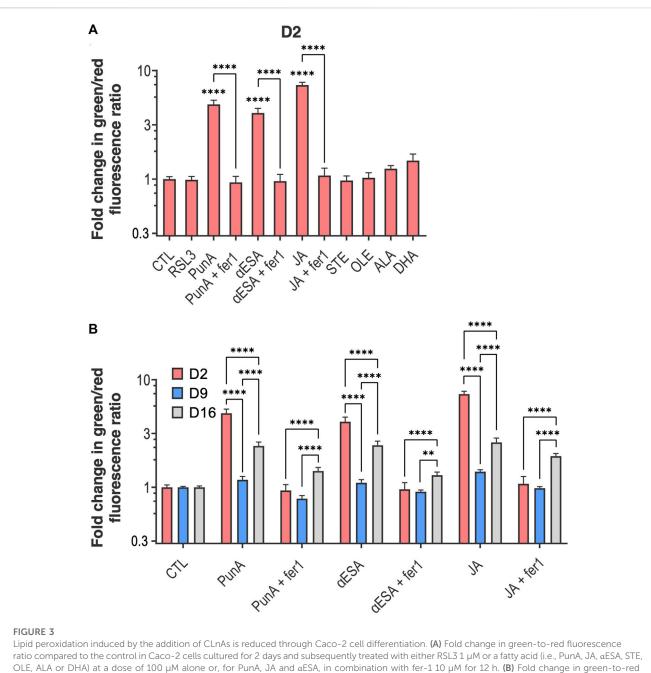
fatty acids with various degrees of unsaturation and chain lengths every second or third day. Over the course of their differentiation, Caco-2 cells progressively developed resistance to the cytotoxicity of all three CLnAs (Figure 2). When exposed to 100 μM PunA, the viability of Caco-2 cells (that was null upon treatment at day 2) amounted to 40% at day 6% and 65% at days 9 to finally reach 85% at day 21, thereby recovering a viability close to the control condition (Figure 2A). Similar trends were observed for the two other CLnAs. The relative viability of Caco-2 cells treated with JA rose from 0% at day 2 to about 70% at days 9 and to more than 85% at day 21 (Figure 2B) while αESA exhibited the strongest and fastest recovery in cell viability according to the time of treatment, going from 8% at day 2%–80% at day 9, and reaching more than 95% at day 21 (Figure 2C). Importantly, the addition of

ferrostatin-1 (fer-1), a ferroptosis inhibitor, prevented the cytotoxicity of CLnAs at all days of cell culture (Figures 2A–C), thereby confirming ferroptosis as the cell death pathway induced by CLnAs in Caco-2 cells. In comparison, the viability of Caco-2 cells exposed to 100 μM RSL3 remained impacted until 17 days of cell differentiation, since it rose from 0% at day 2 to about 80% at day 17, thus at a later time of differentiation compared to CLnAs (Figure 2D). Surprisingly, the addition of fer-1 did not prevent RSL3 cytotoxicity, probably due to the large dose differences of the two compounds (i.e. 100 μM of RSL3 and only 10 μM of fer-1). This suggests that targeting GPX4 as a major antioxidant system is more detrimental to differentiated cells than influencing cellular lipid composition with CLnAs. Interestingly, none of the other tested fatty acids, namely, STE, OLE, ALA and DHA,

FIGURE 2
Caco-2 cells develop resistance to CLnA cytotoxicity throughout their differentiation. **(A–D)** Viability of Caco-2 cells cultured over 21 days and subsequently treated every second or third day with **(A)** PunA, **(B)** JA, **(C)** αESA or **(D)** RSL3 at a dose of 100 µM alone or in combination with fer-1 10 µM. **(E)** Viability of Caco-2 cells cultured over 21 days on which the following treatments have been applied every second of third day: control, STE, OLE, ALA or DHA at 100 µM. Results are expressed as mean ± standard error of the mean of three independent repetitions. Statistical significance is established in relation to the control (i.e., cells cultured in DMEM medium without added fatty acids) (*) or to the addition of a CLnA at each treatment point (#). *#$p <$ 0.05, **##$p <$ 0.01, ***###$p <$ 0.001, ****####$p <$ 0.0001. Abbreviations: ALA, α-linolenic acid; DHA, docosahexaenoic acid; fer-1, ferrostatin-1; OLE, oleic acid; STE, stearic acid; refer to previous Figures for other abbreviations.

was cytotoxic to Caco-2 cells at any time of cell culture (Figure 2D). These results are in line with previous reports on the effect of these fatty acids on cancer cells (Magtanong et al., 2019; Beatty et al., 2021; Dierge et al., 2021) and support
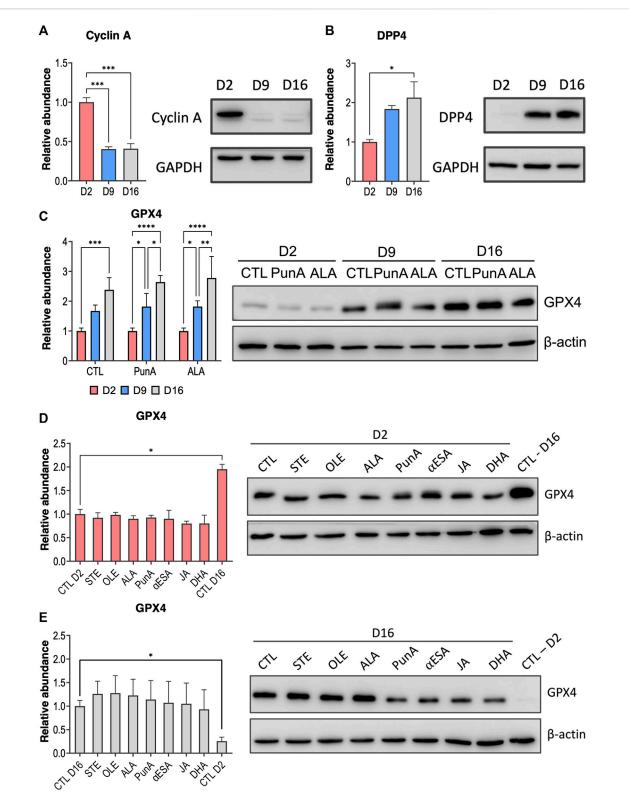
the specific pro-ferroptotic potential of CLnAs. These data also suggest that along their differentiation, enterocyte-like Caco-2 cells progressively develop ferroptosis resistance mechanisms that prevent CLnA cytotoxicity.

FIGURE 3
Lipid peroxidation induced by the addition of CLnAs is reduced through Caco-2 cell differentiation. **(A)** Fold change in green-to-red fluorescence ratio compared to the control in Caco-2 cells cultured for 2 days and subsequently treated with either RSL3 1 μM or a fatty acid (i.e., PunA, JA, αESA, STE, OLE, ALA or DHA) at a dose of 100 μM alone or, for PunA, JA and αESA, in combination with fer-1 10 μM for 12 h. **(B)** Fold change in green-to-red fluorescence ratio compared to the control in Caco-2 cells cultured for either 2, 9 or 16 days and subsequently treated with PunA, JA or αESA at a dose of 100 μM alone or in combination with fer-1 10 μM for 12 h. Results are expressed as mean ± standard error of the mean of three independent repetitions. Statistical significance is established in relation to the control (i.e., cells cultured in DMEM medium without added fatty acid) **(A)**, between the CLnA alone and its combination with fer-1 **(A)** or between the days of cell differentiation for a same treatment **(B)**. ***$p < 0.001$, ****$p < 0.0001$. Refer to previous Figures for other abbreviations.

3.3 CLnA-induced lipid peroxidation is reduced over the course of Caco-2 cell differentiation

We next investigated the effect of CLnAs on lipid peroxidation levels in differentiating Caco-2 cells by using the C11 BODIPY assay (Dierge et al., 2021; Vermonden et al., 2021). We cultured Caco-2 cells for either 2, 9 or 16 days and exposed cells for 12 h to the following conditions: RSL3, STE, OLE, ALA, DHA or a CLnA, either alone or combined with fer-1. At day 2, PunA, JA and αESA induced

respectively a significant 4.9-, 7.3- and 4.1-fold increase in lipid peroxidation compared to the control (Figure 3A). These increases in lipid peroxidation were inhibited by the addition of fer-1, further confirming that CLnAs induce ferroptosis through lipid peroxidation in undifferentiated Caco-2 cells. None of the other tested fatty acids impacted the level of lipid peroxidation compared to the control (Figure 3A). Of note, RSL3 at the dose tested (i.e. 1 μM) did not induce changes in lipid peroxidation in Caco-2 cells at day 2 (Figure 3A). More importantly, CLnA-induced lipid peroxidation was completely abolished in Caco-2 cells at day

FIGURE 4
Caco-2 cells upregulate GPX4 through their differentiation while downregulating proliferation markers. **(A)** Immunoblots and associated relative abundance of cyclin A in Caco-2 cells cultured for either 2, 9 or 16 days. **(B)** Immunoblots and associated relative abundance of DPP4 in Caco-2 cells cultured for either 2, 9 or 16 days. **(C)** Immunoblots and associated relative abundance of GPX4 in Caco-2 cells cultured for either 2, 9 or 16 days and subsequently treated with control, PunA or ALA 100 μM for 24 h. **(D)** Immunoblots and associated relative abundance of GPX4 in Caco-2 cells cultured for either **(D)** 2 or **(E)** 16 days and subsequently treated with control, STE, OLE, ALA, PunA, αESA, JA or DHA 100 μM for 24 h. Relative abundance was calculated based on the ratio of the protein of interest to the protein of reference (i.e., β-actin) and normalized to the control condition (i.e., cells cultured in DMEM medium without added fatty acid). Another control corresponding either to control cells at day 16 or at day 2 has been added to immunoblots performed at day 2 **(D)** or at day 16 **(E)**, respectively. Results are expressed as mean ± standard error of the mean of three independent
(Continued)

FIGURE 4 (Continued)
repetitions. Immunoblots are representative of three independent repetitions. Statistical significance is established in relation to day 2 **(A–C)**, between days 9 and 16 **(C)** or with the negative control **(D–E)**. *$p < 0.05$, **$p < 0.01$, ***$p < 0.001$, ****$p < 0.0001$. Abbreviations: DPP4, dipeptidylpeptidase 4; GPX4, glutathione peroxidase 4; refer to previous Figures for other abbreviations.

---

9 compared to day 2 (Figure 3B). As a result, at day 9, the level of lipid peroxidation in Caco-2 cells treated with a CLnA was not significantly different from the amounts measured at day 2 in the presence of fer-1. None of the other tested fatty acids induced a change in lipid peroxidation between day 2 and day 9 of cell culture (Figure 3B; Supplementary Figure S2). Intracellular lipid peroxidation was slightly but significantly increased in Caco-2 cells treated with either CLnA on day 16 as compared to day 9 (Figure 3B). This difference between days 9 and 16 may be due to the establishment of senescence in long-term cultured Caco-2 cells, which is linked to an overall accumulation of intracellular ROS (Sies and Jones, 2020) and a possible increase in CLnA-induced peroxidation. This hypothesis is supported by a visible increasing trend in the abundance of the p21 senescence marker protein (McHugh and Gil, 2018) in Caco-2 cells at day 16 of their differentiation compared to day 2 (Supplementary Figure S3). Still, altogether our findings support that differentiating enterocytes progressively acquire resistance to CLnA-induced lipid peroxidation and subsequent ferroptosis.

3.4 Resistance to CLnA-induced ferroptosis correlates with increased expression of GPX4

Our results indicate that Caco-2 cells progressively develop CLnA-induced ferroptosis resistance throughout their differentiation in enterocytes. We therefore assumed that resistance to CLnA cytotoxicity would correlate positively with differentiation markers and negatively with proliferation markers. We performed immunoblots on Caco-2 cells cultured for 2, 9 or 16 days. We selected cyclin A, a major regulator of cell cycle and division (Deshpande et al., 2005; Natoli et al., 2011), as a marker of cell proliferation, and dipeptidyl peptidase 4 (DPP4), which is an enzyme expressed at the membrane of differentiated enterocytes (Yoshioka et al., 1991), as a marker of cell differentiation. The abundance of cyclin A significantly dropped at days 9 and 16 of culture of Caco-2 cells, with a 2.5-fold decrease from day 9 compared to day 2 (Figure 4A). On the contrary, DPP4 level in Caco-2 cells increased after 9 days of differentiation and was further upregulated after 16 days of differentiation, with a 2.2-fold rise in abundance at day 16 compared to day 2 (Figure 4B). Taken together, these data confirm that the onset of CLnA-induced ferroptosis resistance coincides with the shift of Caco-2 cells from a proliferative to a differentiated state.

In recent years, multiple studies have highlighted the major role of GPX4 as ferroptosis suppressor, as demonstrated by the induction of ferroptosis when GPX4 is blocked with specific pharmacological inhibitors or by genetic deletion (Seiler et al., 2008; Yang et al., 2014; Hangauer et al., 2017; Viswanathan et al., 2017; Zou et al., 2019). The main role of GPX4 is to protect cells against the deleterious

accumulation of lipid hydroperoxides (Seiler et al., 2008; Yang et al., 2014). Given its major role in ferroptosis, we investigated whether GPX4 is involved in the development of the resistance of differentiating Caco-2 cells to CLnA cytotoxicity. Caco-2 cells showed a progressive increase in GPX4 abundance throughout their differentiation, with a significant 2.4-fold rise at day 16 compared with day 2 (Figure 4C). This increase was similar when Caco-2 cells were exposed to PunA or ALA, showing a 2.6-fold rise in GPX4 abundance at day 16 compared to day 2 (Figure 4C). In fact, when treated with any of the tested fatty acids, GPX4 levels remained unchanged compared to the control, both at day 2 (Figure 4D) and at day 16 of cell differentiation (Figure 4E), indicating that the observed upregulation of GPX4 was not induced in response to CLnAs. Interestingly, while the viability of Caco-2 cells treated with a CLnA did not significantly increase between days 9 and 16 (Figure 2A), GPX4 abundance continuously rose over cell differentiation (Figure 4E), suggesting that lipid peroxide detoxification is already fully insured with a sub-maximal amount of GPX4 in Caco-2 cells. More importantly, Caco-2 cells at day 16 showed again CLnA sensitivity when co-treated with JA and a GPX4 inhibitor (i.e., RSL3) (Supplementary Figure S4A), further emphasizing the major role of GPX4 in protecting Caco-2 cells against CLnA cytotoxicity. Of note, we also assessed changes in the expression of another ferroptosis marker, ACSL4, which preferentially activates PUFAs in their CoA form to incorporate them in phospholipids and which was found to be a ferroptosis initiator (Doll et al., 2017). However, ACSL4 levels remained unchanged between days 2, 9 and 16 of Caco-2 culture (Supplementary Figure S4B), suggesting that ACSL4 is not involved in the development of Caco-2 resistance to CLnA-induced ferroptosis. On the whole, our results indicate that while proliferating Caco-2 cells are sensitive to ferroptosis induced by CLnAs, Caco-2 cells progressively increase their GPX4 protein levels throughout their differentiation in enterocytes, thereby acquiring the detoxification mechanism necessary to prevent ferroptosis.

4 Discussion

Ferroptosis has recently emerged as a cell death pathway that is usually triggered by either inhibition of cystine-glutamate transporter or glutathione peroxidase GPX4. We previously reported another potential manner to induce ferroptosis that is the use of plant-derived CLnAs, which are specific polyunsaturated fatty acids with a higher potential of lipid peroxidation due to their three conjugated double bonds (Vermonden et al., 2021). Here, we show that CLnAs are cytotoxic to proliferating Caco-2 cells by inducing ferroptosis through extensive intracellular lipid peroxidation but spare differentiated enterocyte-like Caco-2 cells.

These results highlight the therapeutic potential of CLnAs with the capacity of this fatty acid subtype to induce tumor growth inhibitory effects while minimizing adverse effects on normal cells.

Since ferroptosis has emerged as a new strategy that may help eradicate therapy-resistant cancer cells (Hangauer et al., 2017; Viswanathan et al., 2017), there has been a growing interest in understanding the regulatory mechanisms behind ferroptotic cell death. However, although a role in tumor suppression and anti-tumor immunity has been suggested (Jiang et al., 2021; Xu et al., 2021), the exact physiological function of ferroptosis remains unclear. Therefore, whether ferroptosis-inducing therapy would be sufficiently specific to cancer cells remains an open and significant question. Here we show that the reduced sensitivity of Caco-2 cells along their differentiation into enterocytes correlates with a reduced extent of lipid peroxidation and an increased expression of the master ferroptosis regulator GPX4. Interestingly, a recent study has shown that immature oligodendrocytes were more susceptible to ferroptosis induced by erastin than differentiated oligodendrocytes due to a higher expression of the cystine/glutamate antiporter and thereby, higher intracellular glutathione concentrations (Hoshino et al., 2020). Another study reported that at a high cell density, the overexpression of E-cadherin by epithelial cells activates the NF2-Hippo pathway, which in turn leads to the inhibition of the pro-ferroptotic YAP transcription factor (Wu et al., 2019). However, we found that E-cadherin expression remained relatively stable over Caco-2 cell differentiation (Supplementary Figure S5), suggesting that while E-cadherin may be involved in ferroptosis resistance in some cell lines, GPX4 upregulation upon cell differentiation is a major mechanism behind the resistance to ferroptosis in enterocyte-like Caco-2 cells. Generally, more work is needed to evaluate whether fast proliferating cells in the body, such as in the bone marrow have also a higher sensitivity to ferroptosis.

Caco-2 cells as a model of enterocyte differentiation has been widely used in the past for drug absorption, barrier permeability and toxicological studies (Hidalgo et al., 1989; Violante et al., 2002; Sambuy et al., 2005). Here, we used Caco-2 cells as a model of differentiating enterocytes in comparison to proliferating cancer cells. Different protocols that allow differentiating human pluripotent stem cells into specific epithelial cells have been developed, such as for endocrine and exocrine pancreatic cells (Gaertner et al., 2019), lung and airway epithelial cells (Huang et al., 2014) and cholangiocytes (Ogawa et al., 2015), among others. Bringing these models together could allow to further explore the link between ferroptosis and cell differentiation across tissues from various origins, and further determine the safety profile of CLnAs but also other types of PUFAs.

References

Beatty, A., Singh, T., Tyurina, Y. Y., Nicolas, E., Maslar, K., Zhou, Y., et al. (2019). Conjugated linolenic fatty acids trigger ferroptosis in triple-negative breast cancer. *bioRxiv*, 556084. doi:10.1101/556084

Beatty, A., Singh, T., Tyurina, Y. Y., Tyurin, V. A., Samovich, S., Nicolas, E., et al. (2021). Ferroptotic cell death triggered by conjugated linolenic acids is mediated by ACSL1. *Nat. Commun.* 12 (1), 2244. doi:10.1038/s41467-021-22471-y

Bian, X., Liu, R., Meng, Y., Xing, D., Xu, D., and Lu, Z. (2021). Lipid metabolism and cancer. *J. Exp. Med.* 218 (1), e20201606. doi:10.1084/jem.20201606

Data availability statement

The original contributions presented in the study are included in the article/Supplementary Material, further inquiries can be directed to the corresponding author.

Author contributions

Conceptualization, GC, PV, and YL; methodology, GC and PV; investigation, GC and PV; resources, RR, OF, and YL; writing—original draft preparation, GC, PV, and YL; writing—review and editing, OF, RR, and YL; visualization, GC and PV; funding acquisition, RR, OF, and YL. All authors have read and agreed to be accountable for the content of the work. All authors contributed to the article and approved the submitted version.

Funding

Conflict of interest

The authors declare that the research was conducted in the absence of any commercial or financial relationships that could be construed as a potential conflict of interest.

Publisher's note

All claims expressed in this article are solely those of the authors and do not necessarily represent those of their affiliated organizations, or those of the publisher, the editors and the reviewers. Any product that may be evaluated in this article, or claim that may be made by its manufacturer, is not guaranteed or endorsed by the publisher.

Supplementary material

The Supplementary Material for this article can be found online at: https://www.frontiersin.org/articles/10.3389/fceld.2023.1219672/full#supplementary-material

Chu, B., Kon, N., Chen, D., Li, T., Liu, T., Jiang, L., et al. (2019). ALOX12 is required for p53-mediated tumour suppression through a distinct ferroptosis pathway. *Nat. Cell. Biol.* 21 (5), 579–591. doi:10.1038/s41556-019-0305-6

Deshpande, A., Sicinski, P., and Hinds, P. W. (2005). Cyclins and cdks in development and cancer: A perspective. *Oncogene* 24 (17), 2909–2915. doi:10.1038/sj.onc.1208618

Dhar Dubey, K. K., Sharma, G., and Kumar, A. (2019). Conjugated linolenic acids: Implication in cancer. *J. Agric. Food Chem.* 67 (22), 6091–6101. doi:10.1021/acs.jafc.9b01379

Dierge, E., Debock, E., Guilbaud, C., Corbet, C., Mignolet, E., Mignard, L., et al. (2021). Peroxidation of n-3 and n-6 polyunsaturated fatty acids in the acidic tumor environment leads to ferroptosis-mediated anticancer effects. *Cell. Metab.* 33 (8), 1701–1715.e5. doi:10.1016/j.cmet.2021.05.016

Dierge, E., Larondelle, Y., and Feron, O. (2020). Cancer diets for cancer patients: Lessons from mouse studies and new insights from the study of fatty acid metabolism in tumors. *Biochimie* 178, 56–68. doi:10.1016/j.biochi.2020.08.020

Dixon, S. J., Lemberg, K. M., Lamprecht, M. R., Skouta, R., Zaitsev, E. M., Gleason, C. E., et al. (2012). Ferroptosis: An iron-dependent form of nonapoptotic cell death. *Cell.* 149 (5), 1060–1072. doi:10.1016/j.cell.2012.03.042

Doll, S., Freitas, F. P., Shah, R., Aldrovandi, M., da Silva, M. C., Ingold, I., et al. (2019). FSP1 is a glutathione-independent ferroptosis suppressor. *Nature* 575 (7784), 693–698. doi:10.1038/s41586-019-1707-0

Doll, S., Proneth, B., Tyurina, Y. Y., Panzilius, E., Kobayashi, S., Ingold, I., et al. (2017). ACSL4 dictates ferroptosis sensitivity by shaping cellular lipid composition. *Nat. Chem. Biol.* 13 (1), 91–98. doi:10.1038/nchembio.2239

Gaertner, B., Carrano, A. C., and Sander, M. (2019). Human stem cell models: Lessons for pancreatic development and disease. *Genes. Dev.* 33 (21–22), 1475–1490. doi:10.1101/gad.331397.119

Hangauer, M. J., Viswanathan, V. S., Ryan, M. J., Bole, D., Eaton, J. K., Matov, A., et al. (2017). Drug-tolerant persister cancer cells are vulnerable to GPX4 inhibition. *Nature* 551 (7679), 247–250. doi:10.1038/nature24297

Hidalgo, I. J., Raub, T. J., and Borchardt, R. T. (1989). Characterization of the human colon carcinoma cell line (Caco-2) as a model system for intestinal epithelial permeability. *Gastroenterology* 96 (3), 736–749. doi:10.1016/s0016-5085(89)80072-1

Hoshino, T., Yamakado, H., Takahashi, R., and Matsuzawa, S. I (2020). Susceptibility to erastin-induced ferroptosis decreases during maturation in a human oligodendrocyte cell line. *FEBS Open Bio* 10 (9), 1758–1764. doi:10.1002/2211-5463.12923

Huang, S. X. L., Islam, M. N., O'Neill, J., Hu, Z., Yang, Y. G., Chen, Y. W., et al. (2014). Efficient generation of lung and airway epithelial cells from human pluripotent stem cells. *Nat. Biotechnol.* 32 (1), 84–91. doi:10.1038/nbt.2754

Jiang, X., Stockwell, B. R., and Conrad, M. (2021). Ferroptosis: Mechanisms, biology and role in disease. *Nat. Rev. Mol. Cell. Biol.* 22 (4), 266–282. doi:10.1038/s41580-020-00324-8

Kagan, V. E., Mao, G., Qu, F., Angeli, J. P. F., Doll, S., Croix, C. S., et al. (2017). Oxidized arachidonic and adrenic PEs navigate cells to ferroptosis. *Nat. Chem. Biol.* 13 (1), 81–90. doi:10.1038/nchembio.2238

Leudeu, B. C. T., Tchiégang, C., Barbé, F., Nicolas, B., and Guéant, J. L. (2009). Ricinodendron heutelotii (Bail) or Tetracarpidium conophorum Müll. oils fed to male rats lower blood lipids. *Nutr. Res. N. Y. N.* 29 (7), 503–509. doi:10.1016/j.nutres.2009.07.004

Liang, C., Zhang, X., Yang, M., and Dong, X. (2019). Recent progress in ferroptosis inducers for cancer therapy. *Adv. Mater Deerf. Beach Fla* 31 (51), e1904197. doi:10.1002/adma.201904197

Magtanong, L., Ko, P. J., To, M., Cao, J. Y., Forcina, G. C., Tarangelo, A., et al. (2019). Exogenous monounsaturated fatty acids promote a ferroptosis-resistant cell state. *Cell. Chem. Biol.* 26 (3), 420–432. doi:10.1016/j.chembiol.2018.11.016

McHugh, D., and Gil, J. (2018). Senescence and aging: Causes, consequences, and therapeutic avenues. *J. Cell. Biol.* 217 (1), 65–77. doi:10.1083/jcb.201708092

Meerts, I. a. T. M., Verspeek-Rip, C. M., Buskens, C. a. F., Keizer, H. G., Bassaganya-Riera, J., Jouni, Z. E., et al. (2009). Toxicological evaluation of pomegranate seed oil. *Food Chem. Toxicol. Int. J. Publ. Br. Ind. Biol. Res. Assoc.* 47 (6), 1085–1092. doi:10.1016/j.fct.2009.01.031

Natoli, M., Leoni, B. D., D'Agnano, I., D'Onofrio, M., Brandi, R., Arisi, I., et al. (2011). Cell growing density affects the structural and functional properties of Caco-2 differentiated monolayer. *J. Cell. Physiol.* 226 (6), 1531–1543. doi:10.1002/jcp.22487

Natoli, M., Leoni, B. D., D'Agnano, I., Zucco, F., and Felsani, A. (2012). Good Caco-2 cell culture practices. *Toxicol. Vitro Int. J. Publ. Assoc. BIBRA* 26 (8), 1243–1246. doi:10.1016/j.tiv.2012.03.009

Ogawa, M., Ogawa, S., Bear, C. E., Ahmadi, S., Chin, S., Li, B., et al. (2015). Directed differentiation of cholangiocytes from human pluripotent stem cells. *Nat. Biotechnol.* 33 (8), 853–861. doi:10.1038/nbt.3294

Pavlova, N. N., and Thompson, C. B. (2016). The emerging hallmarks of cancer metabolism. *Cell. Metab.* 23 (1), 27–47. doi:10.1016/j.cmet.2015.12.006

Perez, M. A., Magtanong, L., Dixon, S. J., and Watts, J. L. (2020). Dietary lipids induce ferroptosis in caenorhabditiselegans and human cancer cells. *Dev. Cell.* 54 (4), 447–454. doi:10.1016/j.devcel.2020.06.019

Sambuy, Y., De Angelis, I., Ranaldi, G., Scarino, M. L., Stammati, A., and Zucco, F. (2005). The caco-2 cell line as a model of the intestinal barrier: Influence of cell and culture-related factors on caco-2 cell functional characteristics. *Cell. Biol. Toxicol.* 21 (1), 1–26. doi:10.1007/s10565-005-0085-6

Seiler, A., Schneider, M., Förster, H., Roth, S., Wirth, E. K., Culmsee, C., et al. (2008). Glutathione peroxidase 4 senses and translates oxidative stress into 12/15-lipoxygenase dependent- and AIF-mediated cell death. *Cell. Metab.* 8 (3), 237–248. doi:10.1016/j.cmet.2008.07.005

Shinohara, N., Tsuduki, T., Ito, J., Honma, T., Kijima, R., Sugawara, S., et al. (2012). Jacaric acid, a linolenic acid isomer with a conjugated triene system, has a strong antitumor effect *in vitro* and *in vivo*. *Biochim. Biophys. Acta BBA - Mol. Cell. Biol. Lipids.* 1821 (7), 980–988. doi:10.1016/j.bbalip.2012.04.001

Sies, H., and Jones, D. P. (2020). Reactive oxygen species (ROS) as pleiotropic physiological signalling agents. *Nat. Rev. Mol. Cell. Biol.* 21 (7), 363–383. doi:10.1038/s41580-020-0230-3

Vermonden, P., Vancoppenolle, M., Dierge, E., Mignolet, E., Cuvelier, G., Knoops, B., et al. (2021). Punicic acid triggers ferroptotic cell death in carcinoma cells. *Nutrients* 13 (8), 2751. doi:10.3390/nu13082751

Violante, G. D., Zerrouk, N., Richard, I., Provot, G., Chaumeil, J. C., and Arnaud, P. (2002). Evaluation of the cytotoxicity effect of dimethyl sulfoxide (DMSO) on caco2/TC7 colon tumor cell cultures. *Biol. Pharm. Bull.* 25 (12), 1600–1603. doi:10.1248/bpb.25.1600

Viswanathan, V. S., Ryan, M. J., Dhruv, H. D., Gill, S., Eichhoff, O. M., Seashore-Ludlow, B., et al. (2017). Dependency of a therapy-resistant state of cancer cells on a lipid peroxidase pathway. *Nature* 547 (7664), 453–457. doi:10.1038/nature23007

Wu, J., Minikes, A. M., Gao, M., Bian, H., Li, Y., Stockwell, B. R., et al. (2019). Intercellular interaction dictates cancer cell ferroptosis via NF2–YAP signalling. *Nature* 572 (7769), 402–406. doi:10.1038/s41586-019-1426-6

Xie, Y., Zhu, S., Song, X., Sun, X., Fan, Y., Liu, J., et al. (2017). The tumor suppressor p53 limits ferroptosis by blocking DPP4 activity. *Cell. Rep.* 20 (7), 1692–1704. doi:10.1016/j.celrep.2017.07.055

Xu, C., Sun, S., Johnson, T., Qi, R., Zhang, S., Zhang, J., et al. (2021). The glutathione peroxidase Gpx4 prevents lipid peroxidation and ferroptosis to sustain Treg cell activation and suppression of antitumor immunity. *Cell. Rep.* 35, 109235. doi:10.1016/j.celrep.2021.109235

Yang, W. H., Ding, C. K. C., Sun, T., Rupprecht, G., Lin, C. C., Hsu, D., et al. (2019). The Hippo pathway effector TAZ regulates ferroptosis in renal cell carcinoma. *Cell. Rep.* 28 (10), 2501–2508. doi:10.1016/j.celrep.2019.07.107

Yang, W. S., SriRamaratnam, R., Welsch, M. E., Shimada, K., Skouta, R., Viswanathan, V. S., et al. (2014). Regulation of ferroptotic cancer cell death by GPX4. *Cell.* 156 (1), 317–331. doi:10.1016/j.cell.2013.12.010

Yoshioka, M., Erickson, R. H., Matsumoto, H., Gum, E., and Kim, Y. S. (1991). Expression of dipeptidyl aminopeptidase IV during enterocytic differentiation of human colon cancer (Caco-2) cells. *Int. J. Cancer* 47 (6), 916–921. doi:10.1002/ijc.2910470622

Zou, Y., Li, H., Graham, E. T., Deik, A. A., Eaton, J. K., Wang, W., et al. (2020). Cytochrome P450 oxidoreductase contributes to phospholipid peroxidation in ferroptosis. *Nat. Chem. Biol.* 16 (3), 302–309. doi:10.1038/s41589-020-0472-6

Zou, Y., Palte, M. J., Deik, A. A., Li, H., Eaton, J. K., Wang, W., et al. (2019). A GPX4-dependent cancer cell state underlies the clear-cell morphology and confers sensitivity to ferroptosis. *Nat. Commun.* 10 (1), 1617. doi:10.1038/s41467-019-09277-9